

**Effect of disorder in MgB<sub>2</sub> thin films**

M. Iavarone, R. Di Capua,\* A. E. Koshelev, and W. K. Kwok  
*Materials Science Division, Argonne National Laboratory, Argonne, Illinois 60439, USA*

F. Chiarella and R. Vaglio  
*INFN-Coherentia Dipartimento di Scienze Fisiche, Facoltà di Ingegneria, Università di Napoli "Federico II," P. le Tecchio 80,  
 80125 Napoli, Italy*

W. N. Kang, E. M. Choi, H. J. Kim, and S. I. Lee  
*NCRICS and Department of Physics, Pohang University of Science and Technology, Pohang 790-784, Republic of Korea*

A. V. Pogrebnnyakov, J. M. Redwing, and X. X. Xi  
*Department of Materials Science and Engineering, The Pennsylvania State University, University Park, Pennsylvania 16802*  
 (Received 30 July 2004; revised manuscript received 24 January 2005; published 2 June 2005)

We report on scanning tunneling spectroscopy studies of magnesium diboride (MgB<sub>2</sub>) thin films grown by different techniques. The films have critical temperatures ranging between 28 and 41 K with very different upper critical fields. We find that the superconducting gap associated with the  $\sigma$  band decreases almost linearly with decreasing critical temperature while the gap associated with the  $\pi$  band is only very weakly affected in the range of critical temperatures above 30 K. In the sample with the lowest critical temperature (28 K) we observe a small increase of the  $\pi$  gap that can only be explained in terms of an increase in the interband scattering. The tunneling data was analyzed in the framework of the two-band model. The magnetic-field-dependent tunneling spectra and the upper critical field measurements of these disordered samples can be consistently explained in terms of an increase of disorder that mostly affects the  $\pi$  band in samples with reduced critical temperatures.

DOI: 10.1103/PhysRevB.71.214502

PACS number(s): 74.70.Ad, 74.50.+r, 74.25.Jb, 68.37.Ef

**I. INTRODUCTION**

The discovery of 40 K superconductivity in magnesium diboride (MgB<sub>2</sub>),<sup>1,2</sup> a compound made of just two light elements, has reinvigorated interest in the fundamental physics of superconductivity. The salient feature in MgB<sub>2</sub> is the existence of two distinct gaps on different portions of the Fermi surface. The two sets of electrons are only weakly interacting and the high  $T_c$  is mainly due to a strong coupling between a small fraction of phonons and a portion of the Fermi surface.<sup>3-5</sup> This is a unique occurrence in superconductors, that did not receive much theoretical and experimental attention earlier. The two-gap scenario in MgB<sub>2</sub> is now commonly accepted in the scientific community and has been investigated by different techniques.<sup>6-14</sup> One of the open issues is the role played by the disorder in a two-band superconductor. Three impurity scattering channels are possible: intraband scattering within each band and interband scattering between them. According to the multiband superconductivity theory<sup>15</sup> the interband scattering by the impurities should blend the order parameters in the two bands, resulting in a merging of the two gaps. The effect of the interband scattering should also decrease the critical temperature expected to be linear in a range of small impurities concentrations.<sup>16,17</sup> Different types of controlled defects have been introduced in this material but, yet no merging of the two gaps has been observed even for samples with substantially reduced critical temperature compared with pure samples. Erwin and Mazin<sup>18</sup> demonstrated that interband scattering  $\sigma$ - $\pi$  is moderately suppressed as a consequence of the spatial symmetry properties

of the electronic states in this material. Only substitutions that cause out-of-plane distortions can lead to significant  $\sigma$ - $\pi$  scattering. Therefore, substitutions in the Mg planes are expected to increase the interband scattering and causing an increase of the  $\pi$  gap and a decrease of the  $\sigma$  gap. In contrast, carbon substitutions, that are expected to affect the  $B$  plane, should give only small contribution to the interband scattering. Point contact spectroscopy experiments and specific-heat experiments<sup>19,20</sup> have confirmed that the two-gap feature persists even in heavily C-doped MgB<sub>2</sub> with a reduced critical temperature as low as 22 K.

We report on a systematic study of tunneling spectroscopy performed by a low-temperature scanning tunneling microscope on thin films, produced by different research groups and grown by different techniques. Our motivation is to study the evolution of the two gaps in this material and elucidate the role of the different scattering channels and their relation with the gap values. The directional nature of tunneling has been used to directly probe the two superconducting gaps. The values of  $\Delta_\sigma$  and  $\Delta_\pi$  that we measured in MgB<sub>2</sub> thin films, with different degree of disorder, have been compared with gap values reported in literature and with new theoretical predictions.<sup>21</sup> Moreover, we demonstrate the existence of two different length scales of the two bands in the presence of a magnetic field. The measured density of states at the Fermi level in the  $\pi$  band approaches the normal value at a field much smaller than the upper critical field  $H_{c2}$  of the sample. The field scale for the gap filling in a presence of magnetic field is set by the ratio of the diffusivities of the quasiparticles in the two bands, while the order parameter

reaches zero at the upper critical field of the sample. We mapped the field dependence of the  $\pi$  band density of states at the Fermi level in films with different degrees of disorder and we fitted the experimental data with the theoretical model proposed by Koshelev and Golubov<sup>17</sup> to extract the diffusivities in the two bands. The combined analysis of the tunneling data and the upper critical field measurements provides a unique tool to better understand and control the disorder in this material.

## II. SAMPLES

We investigated three types of  $\text{MgB}_2$  thin films. The films with the highest critical temperature (film A) were produced at Penn State University by hybrid physical-chemical vapor deposition (HPCVD).<sup>22</sup> X-ray diffraction and transmission electron microscopy indicate that the films are epitaxial on SiC substrates with  $c$  axis oriented normal to the substrate surface.<sup>22</sup> The lattice parameters deduced from x ray are  $c = 3.52 \pm 0.01$  and  $a = 3.09 \pm 0.03$ . From x-ray measurements and from TEM there is no evidence of MgO at the interface with the substrate or at the film's surface. The critical temperature of these films is 41 K, higher than the bulk critical temperature, due to the strain in the films induced by the substrate. The resistivity at low temperature is  $\rho(50 \text{ K}) = 0.26 \mu\Omega \text{ cm}$  and the residual resistivity ratio  $\rho(300 \text{ K})/\rho(40 \text{ K}) = 30$ .

High quality  $c$ -axis oriented  $\text{MgB}_2$  films on (1102)  $\text{Al}_2\text{O}_3$  substrates (films B1 and B2) were grown at Pohang University of Korea using a pulsed laser deposition.<sup>23</sup> X-ray diffraction indicate that most of the grains are oriented with the  $c$ -axis normal to the substrate, but their  $ab$ -plane orientation is relatively random. The surface of the films is  $5 \times 5 \text{ mm}^2$  and the thickness is of the order of 400 nm. The critical temperature of these films typically ranges from 35 to 39 K, with a sharp transition ( $\Delta T_c \approx 0.5 \text{ K}$ ), measured by SQUID magnetometry.<sup>24</sup>

Finally, a third set of films grown by an in situ two step planar magnetron sputtering technique (films C1 and C2),<sup>25</sup> were produced at the INFM Coherencia at the University of Napoli "Federico II." For these samples, x-ray diffraction measurements indicated a broad range of  $c$ -axis orientation. Furthermore, atomic force microscopy (AFM) analysis showed granular features at the surface with average roughness on a single grain being about 20 nm. Scanning electron microscopy (SEM) images with microprobe analysis showed high composition uniformity. The room-temperature resistivity values, estimated using a standard four probe geometry, were fairly high ( $\approx 100 \mu\Omega \text{ cm}$ ), probably due to the granular structure of the films, which affects the estimate of the "effective thickness," due to the limited contact area between the grains. Best samples showed  $T_c = 35 \text{ K}$ ,  $\Delta T_c = 0.5 \text{ K}$  (10–90 % criterion), and residual resistivity ratio  $\rho(300 \text{ K})/\rho(40 \text{ K}) = 1.6$ .

In Fig. 1 SEM images of film A and film C1 are reported. The film A [Fig. 1(a)] consists of hexagonal crystallites of submicron size, mostly oriented along the  $c$  axis. The film C1 [Fig. 1(b)] is much more disordered morphologically. SEM images of films B1 and B2 are reported elsewhere.<sup>26</sup>

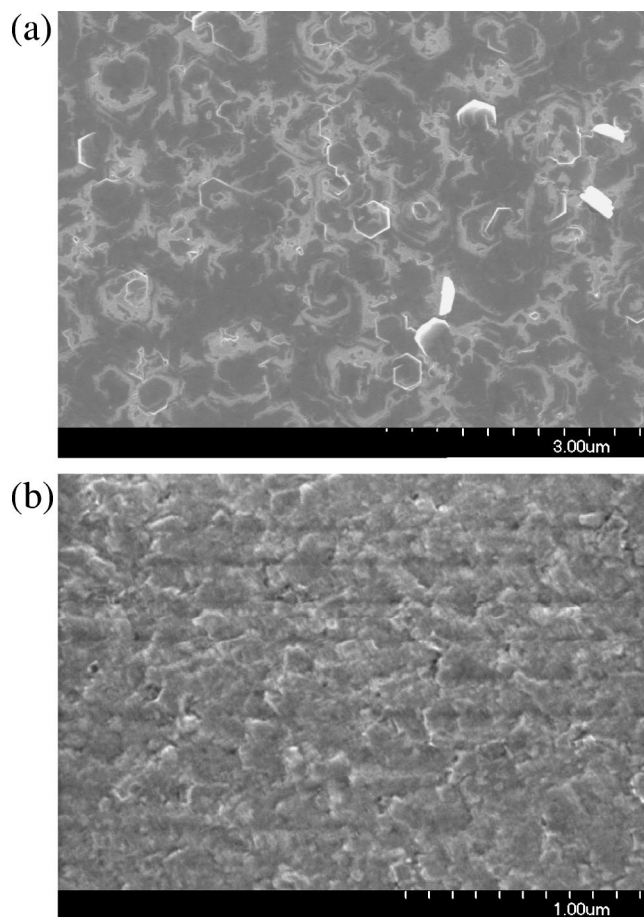


FIG. 1. SEM micrograph of (a) film A and (b) film C2.

The morphology of these films is more similar to film A, with crystallites submicron size.

## III. STM MEASUREMENTS

Tunneling spectroscopic measurements were performed on the as-grown samples at Argonne National Laboratory, using a low-temperature, helium-exchange gas scanning tunneling microscope (STM). In Fig. 2 the STM topographies recorded on films A, B1, B2, and C2 are reported. The topography of film A in Fig. 2(a) shows terraces with steps of the order of 1 nm and roughness on each terrace of 0.1 nm. The topography of film B1 [Fig. 2(b)] is very similar to the one in film A while film B2 in Fig. 2(c) consists of submicron crystallites with the ( $ab$ ) crystallographic plane slightly tilted with respect to the substrate. The topography of film C2 in Fig. 2(d) consists of grains on the order of 100–200 nm in size consistent with the SEM images. Comparing the topography of the four films, C2 is the most disordered morphologically.

Current-voltage characteristics ( $I$ - $V$ ) and conductance spectra ( $dI/dV$  vs  $V$ ) were recorded at different locations on the scanning area. The differential conductance  $dI/dV$  vs  $V$  curves were recorded using a standard lock-in technique with a small ac modulation superimposed on a slowly varying bias voltage while the feedback loop was interrupted. The

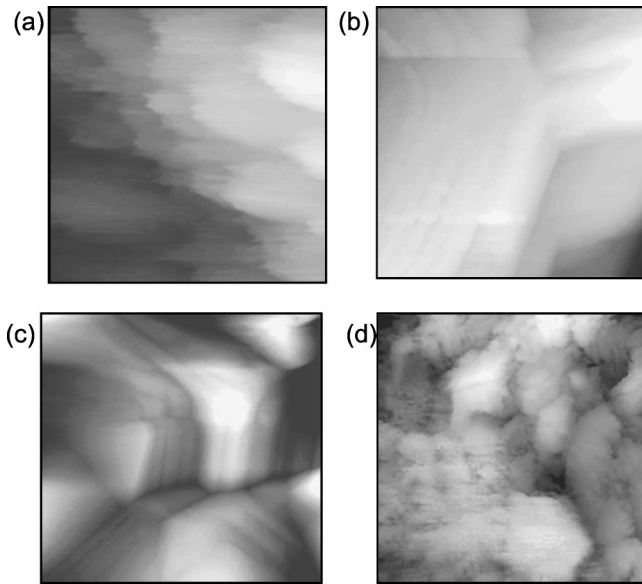


FIG. 2. STM topography of (a) film A, scanning area  $200 \text{ nm} \times 200 \text{ nm}$ , (b) film B1, scanning area  $300 \text{ nm} \times 300 \text{ nm}$ , (c) film B2, scanning area  $300 \text{ nm} \times 300 \text{ nm}$ , (d) film C2, scanning area  $1 \mu\text{m} \times 1 \mu\text{m}$ .

amplitude of the ac modulation was fixed between 0.2 and 0.4 mV, below the intrinsic thermal broadening value at 4.2 K.

As pointed out in our earlier publication,<sup>13</sup> band structure effect in tunneling spectra allows us to probe the two bands in MgB<sub>2</sub> with different weights depending on the tunneling direction. Figures 3(a), 3(b), and 3(c) show two spectra acquired on each sample with critical temperatures  $T_c = 40, 35,$  and  $33.5 \text{ K}$ , respectively. The spectra showing two-gap features were acquired close to a step edge, where tunneling from the side of the tip into the  $a$ - $b$  planes allows us to probe both the  $\sigma$  and  $\pi$  band of this material. In Fig. 3(d) a tunneling spectrum recorded on a  $28 \text{ K}$  sample is reported. On this

film we were not able to observe a clear two gap feature spectrum. Whether the two gaps are present but not resolvable at liquid helium temperature or the disorder in the sample merged the two gaps is still not clear. However, the reduced value of the observed gap  $2\Delta/kT_c$  is well below the BCS weak coupling value of 3.52. Although this is quite unusual and theoretically unexplained, earlier measurements have indicated existence of very low BCS ratio in disordered samples.<sup>27-29</sup>

Figures 4(a) and 4(b) compare  $c$ -axis and off- $c$ -axis tunneling spectra for samples with different  $T_c$ . The large gap associated with the  $\sigma$  band, looks very sensitive to the critical temperature while the changes in the small gap are much smaller. In the sample with lowest  $T_c$  the unprocessed data [Fig. 4(a)] show an increase of the  $\pi$  gap, which can only come from an increase in interband scattering.

The tunneling spectra can be compared to a two-gap tunneling conductance model which is based on a weighted sum of two modified BCS density of states, that includes the effect of the interband scattering, broadened by the Fermi function.<sup>13</sup> The model contains four scattering parameters  $\Gamma_{\sigma\pi}, \Gamma_{\pi\sigma}, \Gamma_{\pi},$  and  $\Gamma_{\sigma}$ . The interband scattering parameters  $\Gamma_{\sigma\pi}$  and  $\Gamma_{\pi\sigma}$  can be reduced to one parameter since their ratio is proportional to the ratio of the density of states at the Fermi level in the two bands, determined from band structure calculations [ $\Gamma_{\sigma\pi}/\Gamma_{\pi\sigma} = N_{\pi}(0)/N_{\sigma}(0)$ ].  $\Gamma_{\pi}$  and  $\Gamma_{\sigma}$  are the intraband scattering parameters. In principle we should consider two different scattering parameters in the two bands, but we considered only one in order to reduce the number of free parameters in our fit, although there is no physical reason to make this assumption. The estimated gap values obtained by comparing the experimental data with the theoretical conductance curves are summarized in Fig. 5(a) together with other gap values reported in the literature. In Fig. 5(b) the BCS ratios for the two gaps are reported and compared with the BCS weak coupling value (straight line) and to data reported by other groups using different techniques (specific heat,<sup>30,31</sup> point contact spectroscopy,<sup>19,32,33</sup> STM) on various

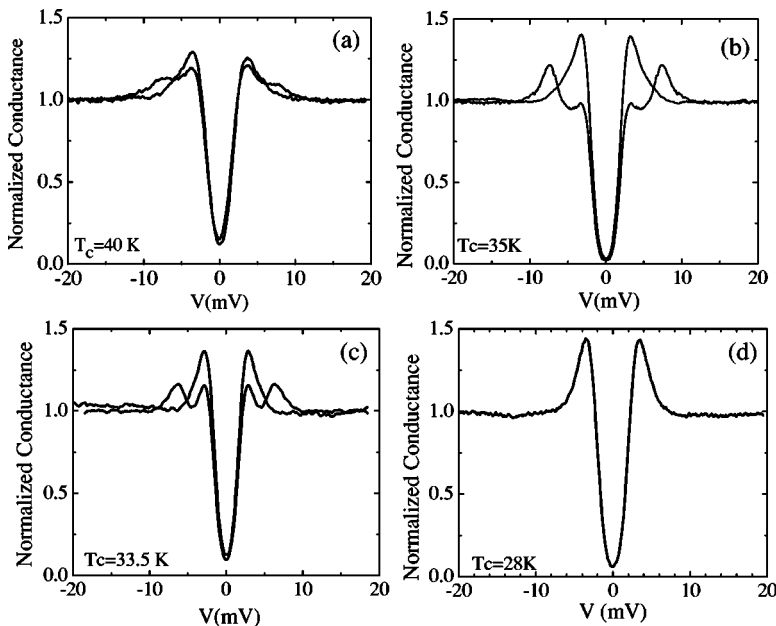


FIG. 3. Tunneling conductance spectra recorded on films with different  $T_c$ , at  $T = 4.2 \text{ K}$ . The tunneling resistance is  $0.2 \text{ G}\Omega$ . The spectra have been normalized to the conductance value at high voltage. For each film the spectrum showing two gap features has been acquired close to a step on the film surface and the one showing one gap far away from steps. (a) Film A, (b) film B2, (c) film C1, (d) film C2.

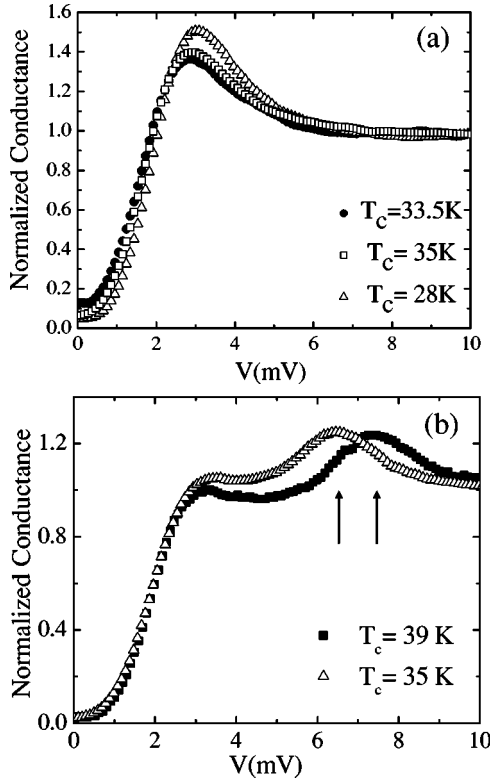


FIG. 4. Tunneling conductance spectra recorded on films with different  $T_c$ , at  $T=4.2$  K. (a)  $c$ -axis spectra on films with  $T_c = 28$  K (film C2), 33.5 K (film C1), and 35 K (film B2). (b) Spectra with  $a$ - $b$  component of the tunneling current, recorded on films with  $T_c = 35$  K (film B2) and 39 K (film B1). The spectra have been normalized to the conductance value at high voltage. The tunneling resistance is  $R_T = 0.2$  G $\Omega$  ( $I = 100$  pA,  $V = 20$  mV).

types of samples (single crystals, bulks, and thin films) where the disorder was introduced in several ways (aluminum substitutions,<sup>31,34</sup> carbon substitutions,<sup>19,32,33</sup> neutron irradiation<sup>30</sup>). Despite the wide variation of the source of disorder it appears that the changes in gap values can be well described by the sample's critical temperature. The gap associated with the  $\pi$  band is only weakly sensitive to the critical temperature in the range of critical temperature 30–39 K while the  $\sigma$  gap decreases almost linearly. The gap values  $\Delta_\pi$  and  $\Delta_\sigma$  form two branches when plotted as a function of the critical temperature of the sample and remarkably, all the published gap values fall on the same two branches. It is important to keep in mind that the reduction in  $T_c$  due to disorder can be caused by an increase of the interband scattering or by a change in the electronic structure that affects the electron-phonon coupling matrix. The decrease of  $\Delta_\sigma$  and the almost constant or slightly increasing value of  $\Delta_\pi$  are consistent with recent theoretical predictions.<sup>21</sup> The model is based on the scaling of the electron-phonon coupling constant and includes effects due to the increase of the interband scattering. Both effects can capture most of the experimental observations.

Up to now, the situation below 30 K remains experimentally more ambiguous. Some experiments<sup>34</sup> report little increase of the  $\pi$  gap, but overall it looks as though the two-

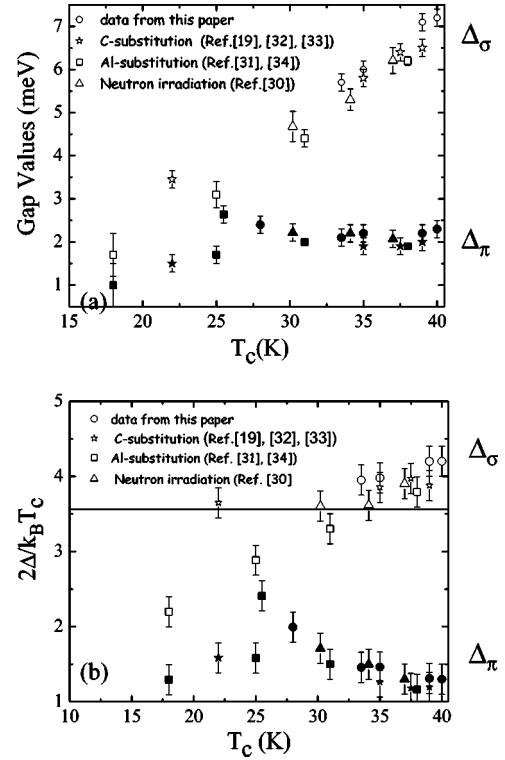


FIG. 5. (a) Gap values for films with different  $T_c$  compared with values reported in literature. (b) BCS ratios obtained from the gap values in (a) and compared with other data reported in literature.

gap feature persists to temperatures very close to 20 K. In particular for C-doped samples with  $T_c = 22$  K there is evidence from specific-heat measurements<sup>20</sup> of the two-gap feature, although the value of this gap is more difficult to extract than from tunneling experiments. Recently, Holanova *et al.*<sup>19</sup> reported point contact spectroscopy on heavily doped C-doped MgB<sub>2</sub> pellets. The existence of the two gaps is very difficult to observe directly from the data (for the  $T_c = 22$  K sample) but after fitting, they were able to determine the values of the two gaps. Gonnelli *et al.*<sup>35</sup> reported a systematic study of the energy gaps in a series of Al-substituted and C-substituted MgB<sub>2</sub> single crystals. They claim that the doping dependence of the gaps is very different for the two series, in particular for heavily doped samples. Indeed, they observed a merging of the two gaps for C-doped samples with  $T_c = 20$  K while they could still resolve a two-gap feature for Al-substituted samples with similar critical temperatures.

#### IV. UNDERSTANDING THE ORIGIN OF DISORDER FROM TUNNELING MEASUREMENTS

In the framework of the two-gap model, it is possible to calculate the change in critical temperature  $T_c$  and the gap values  $\Delta_\pi$  and  $\Delta_\sigma$  as a function of the interband scattering:

$$\delta T_c = - \frac{\pi \Gamma_{\sigma\pi} (W_\pi - W_{\sigma\pi}) + \Gamma_{\sigma\pi} (W_\pi - W_{\pi\sigma})}{8 W_\sigma + W_\pi},$$

$$\delta\Delta_\sigma = \frac{\Gamma_{\sigma\pi} \Delta_\pi - \Delta_\sigma}{2 \Delta_\sigma} \frac{R\left(\frac{\Delta_\pi}{\Delta_\sigma}\right) \left( W_\pi + \ln \frac{\Delta_\pi}{\alpha T_c} + 1 \right) - \frac{\Delta_\sigma}{\Delta_\pi} R\left(\frac{\Delta_\sigma}{\Delta_\pi}\right) W_{\pi\sigma}}{W_\sigma + W_\pi + \ln \frac{\Delta_\pi}{\alpha T_c} + \ln \frac{\Delta_\sigma}{\alpha T_c} + 1},$$

$$\delta\Delta_\pi = \frac{\Gamma_{\pi\sigma} \Delta_\sigma - \Delta_\pi}{2 \Delta_\pi} \frac{R\left(\frac{\Delta_\sigma}{\Delta_\pi}\right) \left( W_\sigma + \ln \frac{\Delta_\sigma}{\alpha T_c} + 1 \right) - \frac{\Delta_\pi}{\Delta_\sigma} R\left(\frac{\Delta_\pi}{\Delta_\sigma}\right) W_{\sigma\pi}}{W_\sigma + W_\pi + \ln \frac{\Delta_\pi}{\alpha T_c} + \ln \frac{\Delta_\sigma}{\alpha T_c} + 1},$$

where

$$R(r) = \int_0^\infty dx \frac{\tanh^2 x}{\sqrt{r^2 + \sinh^2 x}},$$

$$R(0) = 1, R(1) = \pi/4, R(r) \approx \frac{\ln 4r - 1}{r} \text{ for } r \gg 1$$

$\alpha$  is the BCS ratio  $2\Delta/k_B T_c$ , the interband scattering  $\Gamma_{\alpha\beta}$  is defined as twice the value of the interband scattering in Ref. 16 and  $W$  is a matrix related to the electron-phonon constants [16].

In the limit of small interband scattering we can consider the linear approximations

$$\delta T_c \approx 0.39 \Gamma_{\sigma\pi}, \quad (1)$$

$$\delta \Delta_\pi \approx 0.23 \Gamma_{\sigma\pi}, \quad (2)$$

$$\delta \Delta_\sigma \approx -0.38 \Gamma_{\sigma\pi}. \quad (3)$$

Since in the low  $T_c$  sample we observe an increase of the  $\Delta_\pi$  of 0.2 meV, from Eqs. (1) and (2), this translates to a decrease in  $T_c$  due to interband scattering of almost 4.6 K. Therefore, not all the decrease in  $T_c$  can be explained in terms of interband scattering. The origin of disorder in thin films is still a matter of debate. In TEM measurements, Gurevich *et al.*<sup>36</sup> observed a buckling of the Mg plane in highly disordered films. Such out-of-plane distortions can increase the interband scattering.

To understand the nature of disorder in these films we focused on the magnetic field dependence of the tunneling spectra. Magnetic field dependence of the tunneling spectra has been reported by many groups either from STM experiments and point-contact spectroscopy. It is well established that the zero bias of the  $c$ -axis tunneling spectra increases with the applied magnetic field quite rapidly. Koshelev and Golubov<sup>17</sup> calculated the local density of states in the presence of a magnetic field for a two-band superconductor and demonstrated that the field dependence of the averaged density of states at the Fermi energy is a function of the ratio of the in-plane diffusivities in the two bands. Figure 6(a) shows the zero bias values of the tunneling spectra at different fields as a function of the normalized upper critical field (at low temperature) in the  $c$ -direction for each sample. According to

the theoretical model proposed by Koshelev and Golubov<sup>17</sup> the slope of the initial increase of the zero bias should decrease when increasing the ratio  $D_\sigma/D_\pi$ , where  $D_\sigma$  and  $D_\pi$  are the diffusivities in the  $ab$  plane of the two bands  $\sigma$  and  $\pi$ , respectively. In our measured samples, it appears that a decrease in  $T_c$  is accompanied with an increase in the ratio  $D_\sigma/D_\pi$ . The experimental data can be compared with the theoretical curves to obtain the ratio of the diffusivities. In Fig. 6(b) the experimental data for the samples with  $T_c=40$ , 35, and 28 K are compared with the calculated curves obtained for  $D_\sigma/D_\pi=0.1, 0.2$ , and 1.5, respectively. The experiment is in good agreement with the theory for samples with high  $T_c$  and marginal for the sample with the lowest  $T_c$ . It is important to keep in mind that the theory does not include the effects of interband scattering that are small but finite in most disordered samples (as shown by the increase of the value of the  $\pi$  gap). Moreover, all the calculations are based

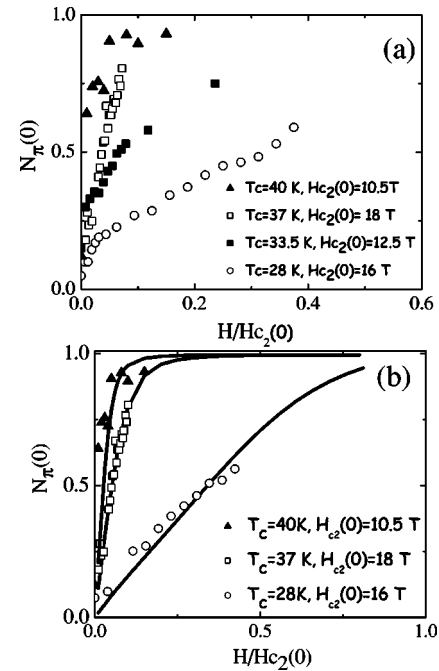


FIG. 6. (a) Zero bias conductance as a function of the applied magnetic field normalized to the upper critical field at zero temperature. (b) Comparison between experimental data and theoretical curves.

TABLE I. Summary of the critical temperature  $T_c$ ; gap values  $\Delta_\pi$ ,  $\Delta_\sigma$ ; extrapolation at zero temperature of the upper critical field for field applied perpendicular to the film surface  $H_{c2}(0)$ ; the ratio of the in plane diffusivities  $D_\sigma/D_\pi$ , evaluated by the comparison between experimental data and theoretical curves [Figs. 4(a) and 4(b)]; and values of the two in plane diffusivities  $D_\sigma$  and  $D_\pi$ . Film A was grown by HPCVD. Films B1 and B2 were grown by the pulsed laser deposition technique. Films C1 and C2 were grown by the magnetron sputtering technique.

	$T_c$ (K)	$\Delta_\pi$ (meV)	$\Delta_\sigma$ (meV)	$H_{c2}(0)$ (T)	$D_\sigma/D_\pi$	$D_\sigma$ (cm <sup>2</sup> /s)	$D_\pi$ (cm <sup>2</sup> /s)
Film A	40±0.1	2.2±0.2	7.2±0.2	10.5±0.5	0.1±0.05	2.7	27
Film B1	39±0.5	2.2±0.2	7.1±0.2	16±0.5	0.2±0.1	1.8	9.0
Film B2	35±0.5	2.2±0.2	6.0±0.2	18±0.5	0.2±0.1	1.4	7.0
Film C1	33.5±0.5	2.0±0.2	5.7±0.2	12.5±0.5	0.3±0.2	2.0	6.0
Film C2	28±0.5	2.4±0.2		16±0.5	1.5±0.4	1.3	0.9

on the electron-phonon coupling matrix obtained from band structure calculations on optimal samples. In disordered samples, this matrix could in principle be very different from optimally grown samples.

The tunneling measurements in the framework of this analysis can only provide an estimate of the ratio of the diffusivities in the  $ab$  plane. To separate the two diffusivities, upper critical field measurements are necessary. It is possible to calculate  $D_\sigma$  from the following equations:<sup>37</sup>

$$g(r_x) = -\frac{W_\sigma + W_\pi - \ln r_x}{2} + \sqrt{\frac{(W_\sigma + W_\pi - \ln r_x)^2}{4} + W_\sigma + \ln r_x},$$

where  $r_x$  is the ratio of the in-plane diffusivities

$$r_x = \frac{D_\sigma}{D_\pi}.$$

$$H_{c2}(0) = 0.14 \frac{2k_B T_c \Phi_0}{\hbar D_\sigma} e^{g(r_x)}, \quad (4)$$

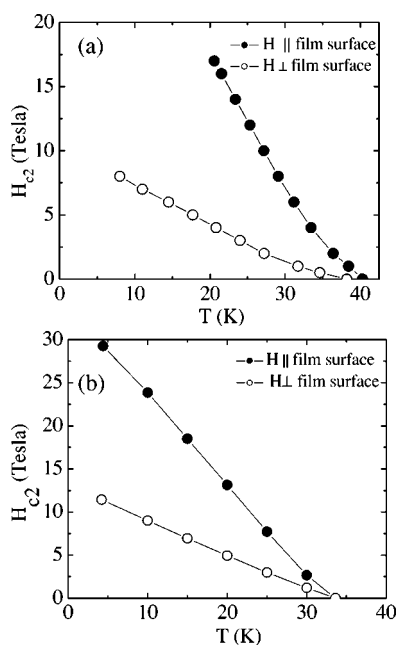


FIG. 7. Upper critical field for  $H$  applied parallel and perpendicular to the film surface for (a) a sample with  $T_c=40$  K (film A), (b) a sample with  $T_c=33.5$  K (film C1).

In Table I the  $T_c$ , gap values,  $H_{c2}(0)$ , diffusivity ratios, and in-plane diffusivities are summarized for the measured samples.  $H_{c2}(0)$  is the upper critical field for magnetic field applied perpendicular to the film surface and it represents the value at zero temperature extrapolated from the experimental data at higher temperatures. Although the estimates of the in plane diffusivities have been made using a model based on the electron-phonon matrix obtained from the band structure calculations for pure MgB<sub>2</sub>, there are some qualitative conclusions that can be drawn from this analysis. For the lowest  $T_c$  film the  $\pi$  band looks dirtier than the  $\sigma$  band while in thin films with higher critical temperatures the  $\pi$  band looks cleaner than the  $\sigma$  band. These conclusions are in agreement with magnetic field measurements performed on the same samples. In Figs. 7(a) and 7(b) we report the upper critical field for two samples with  $T_c=40$  and 33.5 K, respectively. According to Gurevich,<sup>38</sup> if the  $\sigma$  band is dirtier than the  $\pi$  band, the plot of the upper critical field  $H_{c2}(T)$ , for  $H$  applied perpendicular to the film surface, should show a positive curvature at  $T_c$ , whereas if the  $\sigma$  band is cleaner than the  $\pi$  band,  $H_{c2}$  vs  $T$  is linear near  $T_c$ . Since the  $\pi$  band is affected by the disorder in the Mg plane, it seems that the reduction of the critical temperature is mainly caused by the disorder in the Mg plane. This is also consistent with the small increase of the interband scattering in the film with  $T_c=28$  K.

In conclusion, we performed a systematic study of tunneling spectroscopy in thin films grown by different techniques to investigate the evolution of the two-gap feature in films with different critical temperatures. We obtained an estimate of the in-plane diffusivities in the two bands through a comparison of the magnetic field dependence of the spectra with the two-band model in disordered films. We find that the

disorder seems to affect mostly the  $\pi$  band in films with reduced critical temperatures.

### ACKNOWLEDGMENTS

This work was supported by US DOE Basic Energy Science–Material Science under Contract No. W-31-109-ENG-38. The authors would like to thank U. Welp, A. Rydh,

and C. Ferdeghini for transport measurements. The work at Penn State is partially supported by ONR under Grants No. N00014-00-1-0294 (Xi) and N0014-01-1-0006 (Redwing) and by NSF under Grant No: DMR-0306746 (Xi and Redwing). Part of this work was carried out in the Electron Microscopy Center at Argonne National Laboratory, which is supported by the DOE Office of Science under Contract No. W-31-109-Eng-38.

- 
- \*Present address: INFM-Coherentia Dipartimento di Scienze Fisiche, Facolta di Ingegneria, Universita' di Napoli "Federico II," P. le Tecchio 80, 80125 Napoli, Italy
- <sup>1</sup>J. Nagamatsu, N. Nakagawa, T. Muranaka, Y. Zenitani, and J. Akimitsu, *Nature (London)* **410**, 63 (2001)
  - <sup>2</sup>A comprehensive review on magnesium diboride can be found in P. C. Canfield and G. W. Crabtree, *Phys. Today* **86**, 34 (2003), and the references within.
  - <sup>3</sup>J. Kortus, I. I. Mazin, K. D. Belashchenko, V. P. Antropov, and L. L. Boyer, *Phys. Rev. Lett.* **86**, 4656 (2001).
  - <sup>4</sup>J. M. An and W. E. Pickett, *Phys. Rev. Lett.* **86**, 4366 (2001).
  - <sup>5</sup>H. J. Choi, D. Roundy, H. Sun, M. L. Cohen, and S. G. Louie, *Nature (London)* **418**, 758 (2002).
  - <sup>6</sup>F. Bouquet, R. A. Fisher, N. E. Phillips, D. G. Hinks, and J. D. Jorgensen, *Phys. Rev. Lett.* **87**, 047001 (2001).
  - <sup>7</sup>Y. Wang, T. Plackonwski, and A. Junod, *Physica C* **355**, 179 (2001).
  - <sup>8</sup>G. Karapetrov, M. Iavarone, W. K. Kwok, G. W. Crabtree, and D. G. Hinks, *Phys. Rev. Lett.* **86**, 4374 (2001).
  - <sup>9</sup>G. Rubio-Bollinger, H. Suderow, and S. Vieira, *Phys. Rev. Lett.* **86**, 5582 (2001).
  - <sup>10</sup>F. Giubileo, D. Roditchev, W. Sacks, R. Lamy, D. X. Thanh, J. Klein, S. Miraglia, D. Fruchart, J. Marcus, and Ph. Monod, *Phys. Rev. Lett.* **87**, 177008 (2001).
  - <sup>11</sup>P. Szabo, P. Samuely, J. Kacmarcik, T. Klein, J. Marcus, D. Fruchart, S. Miraglia, C. Marcenat, and A. G. M. Jansen, *Phys. Rev. Lett.* **87**, 137005 (2001).
  - <sup>12</sup>H. Schmidt, J. F. Zasadzinski, K. E. Gray, and D. G. Hinks, *Phys. Rev. Lett.* **88**, 127002 (2002).
  - <sup>13</sup>M. Iavarone, G. Karapetrov, A. E. Koshelev, W. K. Kwok, G. W. Crabtree, D. G. Hinks, W. N. Kang, E. M. Choi, H. J. Kim, H. J. Kim, and S. I. Lee, *Phys. Rev. Lett.* **89**, 187002 (2002).
  - <sup>14</sup>M. R. Eskildsen, M. Kugler, S. Tanaka, J. Jun, S. M. Kazakov, J. Karpinski, and O. Fischer, *Phys. Rev. Lett.* **89**, 187003 (2002).
  - <sup>15</sup>H. Suhl, B. T. Matthias, and L. R. Walker, *Phys. Rev. Lett.* **3**, 552 (1959).
  - <sup>16</sup>V. Braccini, A. Gurevich, J. E. Giencke, M. C. Jewell, C. B. Eom, D. C. Larbalestier, A. Pogrebnnyakov, Y. Cui, B. T. Liu, Y. F. Hu, J. M. Redwing, Qi Li, X. X. Xi, R. K. Singh, R. Gandikota, J. Kim, B. Wilkens, N. Newman, J. Rowell, B. Moeckly, V. Ferrando, C. Tarantini, D. Marre, M. Putti, C. Ferdeghini, R. Vaglio, and E. Haanappel, *cond-mat/0402001* (unpublished).
  - <sup>17</sup>A. E. Koshelev and A. A. Golubov, *Phys. Rev. Lett.* **90**, 177002 (2003).
  - <sup>18</sup>S. C. Erwin and I. I. Mazin, *Phys. Rev. B* **68**, 132505 (2003).
  - <sup>19</sup>Z. Holanava, P. Szabo, P. Samuely, R. H. T. Wilke, S. L. Bud'ko, and P. C. Canfield, *cond-mat/0404096* (unpublished).
  - <sup>20</sup>R. A. Ribeiro, S. L. Bud'ko, C. Petrovic, and P. C. Canfield, *Physica C* **384**, 227 (2003).
  - <sup>21</sup>J. Kortus, O. V. Dolgov, R. K. Kremer, and A. A. Golubov, *Phys. Rev. Lett.* (to be published), *cond-mat/0411667*
  - <sup>22</sup>X. H. Zeng, A. V. Pogrebnnyakov, A. Kotcharov, J. E. Jones, X. X. Xi, E. M. Lysczek, J. M. Redwing, S. Y. Xu, J. Lettieri, D. G. Schlom, W. Tian, X. Q. Pan, and Z. K. Liu, *Nat. Mater.* **1**, 35 (2002).
  - <sup>23</sup>W. N. Kang, Hyeong-Jin Kim, Eun-Mi Choi, C. U. Jung, and S. I. Lee, *Science* **292**, 1521 (2001).
  - <sup>24</sup>W. N. Kang, Eun-Mi Choi, Hyeong-Jin Kim, and S. I. Lee, *Physica C* **385** 24 (2003).
  - <sup>25</sup>R. Vaglio, M. G. Maglione, and R. Di Capua, *Supercond. Sci. Technol.* **15**, 1236 (2002).
  - <sup>26</sup>M. Iavarone, G. Karapetrov, A. E. Koshelev, W. K. Kwok, G. W. Crabtree, W. N. Kang, E. M. Choi, H. j. Kim, and S. I. Lee, *Supercond. Sci. Technol.* **17**, S106 (2004).
  - <sup>27</sup>C. Camerlingo, P. Scardi, C. Tosello, and R. Vaglio *Phys. Rev. B* **31**, 3121 (1985).
  - <sup>28</sup>T. H. Geballe, *Advances in Superconductivity*, edited by B. Deaver and J. Ruvalds, vol. 100 of NATO Advanced Study Institute, Series B: Physics (Plenum, New York, 1982), p. 387.
  - <sup>29</sup>K. Tanabe, H. Asano, and O. Michikami, *Appl. Phys. Lett.* **44**, 559 (1984).
  - <sup>30</sup>Y. Wang, F. Bouquet, I. Sheikin, P. Toulemonde, B. Revaz, M. Eisterer, H. W. Weber, J. Hinderer, and A. Junod, *J. Phys.: Condens. Matter* **15**, 883 (2003).
  - <sup>31</sup>M. Putti, M. Affronte, P. Manfrinetti, and A. Palenzona, *Phys. Rev. B* **68**, 094514 (2003).
  - <sup>32</sup>H. Schmidt, K. E. Gray, D. G. Hinks, J. F. Zasadzinski, M. Avdeev, J. D. Jorgensen, and J. C. Burley, *Phys. Rev. B* **68**, 060508(R) (2003).
  - <sup>33</sup>P. Samuely, Z. Holanava, P. Szabo', J. Kacmarcik, R. A. Ribeiro, S. L. Bud'ko, and P. C. Canfield, *Phys. Rev. B* **68**, 020505(R) (2003).
  - <sup>34</sup>M. Eskildsen (unpublished).
  - <sup>35</sup>R. S. Gonnelli, D. Daghero, G. A. Ummarino, A. Calzolari, V. Dellarocca, V. A. Stepanov, S. M. Kazakov, J. Jun, and J. Karpinski, *cond-mat/0407267* (unpublished).
  - <sup>36</sup>A. Gurevich, S. Patnaik, V. Braccini, K. H. Kim, C. Mielke, X. Song, L. D. Cooley, S. D. Bu, D. M. Kim, J. H. Choi, L. J. Belenky, J. Giencke, M. K. Lee, W. Tian, X. Q. Pan, A. Siri, E. E. Hellstrom, C. B. Eom, and D. C. Larbalestier, *cond-mat/0305474* (unpublished).
  - <sup>37</sup>A. A. Golubov and A. E. Koshelev, *Phys. Rev. B* **68**, 104503 (2003).
  - <sup>38</sup>A. Gurevich *Phys. Rev. B* **67**, 184515 (2003).